

JPL Document D-XXXXX



TPF-I Technology Milestone #3 Whitepaper Broadband Starlight Suppression Demonstration

Editors:

P. R. Lawson, R. O. Gappinger, R. D. Peters, and O. P. Lay

October 10, 2007

National Aeronautics and Space Administration

**Jet Propulsion Laboratory
California Institute of Technology
Pasadena, California**

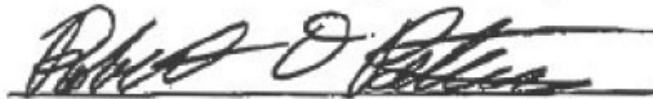
Approvals

Released by



 Robert O. Gappinget,
 TPF-I Achromatic Nulling Testbed Cog. E.

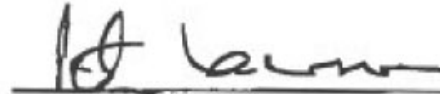
10/03/07



 Robert D. Peters,
 TPF-I Adaptive Nuller Cog. E.

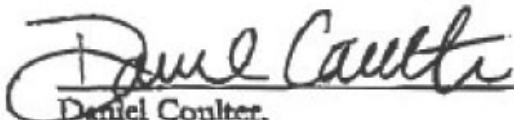
10/3/2007

Approved by



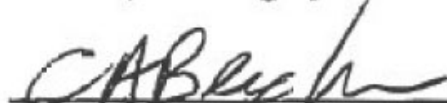
 Peter R. Lawson,
 TPF-I Systems Manager

10/3/2007



 Daniel Coulter,
 TPF Project Manager JPL

10/8/07



 Charles Beichman,
 TPF-I Project Scientist, JPL

10/7/2007



 Michael Devirian
 Navigator Program Manager, JPL

10/07/07



 Zlatan Tsvetanov
 TPF Program Scientist, NASA HQ

10/09/2007



 Lia LaPiana
 TPF Program Executive, NASA HQ

10/9/07

Table of Contents

Approvals.....iii

Table of Contents iv

1. Objective1

2. Introduction1

 2.1. Achromatic Nulling Testbed2

 2.2. Adaptive Nuller.....6

 2.3. Differences between Flight and Lab Demonstration7

3. Milestone Procedure: Achromatic Nulling Testbed..... 8

 3.1. Definitions8

 3.2. Measurement of the null.....9

 3.3. Milestone #3 Validation Procedure.....9

4. Milestone Procedure: Adaptive Nuller.....10

 4.1. Definitions10

 4.2. Measurement of the null.....12

 4.3. Milestone #3 Validation Procedure.....12

5. Success Criteria13

6. Certification Process14

 6.1. Certification Data Package.....14

7. References14

Terrestrial Planet Finder Interferometer

TPF-I Technology Milestone #3 Whitepaper

Broadband Starlight Suppression Demonstration

1. Objective

In support of the Terrestrial Planet Finder Interferometer (TPF-I) pre-phase-A development program, this white paper explains the purpose of TPF-I Technology Milestone #3, specifies the methodology for computing the milestone metric, and establishes the success criteria against which the metric will be evaluated.

2. Introduction

The intent of this technology milestone was established in the TPF-I Technology Plan (JPL Pub. 05-5, June 2005) to gauge the developmental progress of the TPF-I project and its readiness to proceed from pre-Phase A to Phase A. Completion of this milestone is to be documented by the project, reviewed by the EIRB, and approved by NASA HQ. The milestone described here addresses broadband starlight suppression.

Milestone #3: Broadband Starlight Suppression

Using either the Adaptive Nuller or the Achromatic Nulling Testbed, demonstrate that mid-infrared light in the 7–12 μm range can be suppressed by a factor of $\geq 10^5$ over a waveband of $\geq 25\%$. This demonstrates the approach to broadband starlight suppression (dimming of light across a range of wavelengths) needed to characterize terrestrial planets for habitability. Flight-like nulls are to be demonstrated at room (non-flight) temperature. *Milestone TRL 5.*

The 10^5 suppression requirement is sufficient to reduce the residual starlight photon rate to below the background level set by the local zodiacal emission. Since the sun-earth flux ratio is $\sim 10^7$ at 10 μm , further rejection is necessary to achieve a detection. This additional rejection is realized through a combination of phase chopping, the fact that the residual starlight is diluted over many pixels in the synthesized image, and the use of a spectral fitting technique that isolates the planet signal (Lay 2006). This additional rejection will be demonstrated by the Planet Detection Testbed.

The two-beam nuller is the basic building block of all flight architectures that have been considered so far. Four approaches to achromatic phase shifting have been investigated, with the aim of demonstrating, through one of the approaches, two-beam nulling to a level of 1 part in 100,000 with a 25% bandwidth. These methods are as follows: (1) using pairs of dispersive glass plates to introduce a wavelength-dependent delay; (2) using a through-focus field-flip of the light in one arm of the interferometer; (3) using successive and opposing field-reversals on reflection off flat mirrors in a periscope arrangement; and (4) through adaptive nulling. The first two methods were tested in the Achromatic Nulling Testbed (ANT) prior to 2006, but yielded null depths no greater than $\sim 1 \times 10^4$. Since that time the third approach has been developed for the ANT using periscope mirrors to im-

prove on these results. The fourth approach, adaptive nulling, was the subject of TPF-I Milestone #1 to demonstrate mid-infrared amplitude and phase compensation over a broad band.

Both the ANT and the Adaptive Nuller approaches will work toward this milestone, but success by either one is sufficient to meet the goal. The ANT was specifically designed to demonstrate Milestone #3, however the Adaptive Nuller has demonstrated deeper nulls (yielding 1.2×10^{-5} in May of 2007) and may ultimately prove to be the more viable approach. The Adaptive Nuller was described in detail in the TPF-I Milestone #1 whitepaper and report, and is only briefly reviewed here. The Achromatic Nulling Testbed is introduced and described in greater depth, below.

Note that all designs under consideration for TPF-I include a single-mode spatial filter through which the combined light is passed before being detected. The wavefront from the star is incident on the collecting apertures of the instrument and delivered by the respective beam trains to a central beam combiner that couples the combined light into a single-mode filter. With just a single mode for each polarization state, the problem of nulling the on-axis light is simplified. Higher order wavefront aberrations that would reduce the visibility of the fringes (depth of the null) are rejected by the spatial filter. Small errors in tilt in each arm of the interferometer thus translate into small errors in received intensity. Neither the Achromatic Nulling Testbed nor the Adaptive Nuller need to adjust wavefront errors across each pupil, as these are rejected independently by the spatial filter. For further information about the mid-infrared spatial filters to be used with TPF-I, the interested reader is referred to Ksendzov *et al.* (2006).

2.1. Achromatic Nulling Testbed

The Achromatic Nulling Testbed (ANT) was designed specifically to develop methods of achieving an achromatic π phase shift and demonstrate deep, broadband, two-beam mid-infrared nulling.

Achromatic Phase Shift: Nulling interferometry requires a π phase shift to be introduced between two interfering beams. In the periscope architecture used in the ANT, the phase shift is accomplished through an electric field flip (or pupil inversion) of one pupil relative to the other within a periscope arrangement of mirrors, as shown in Fig. 1. The periscope layout is fully symmetric, and because of the geometric nature of the field flip, the π phase shift is intrinsically achromatic. The field inversion periscope is composed of four mirrored prisms optically bonded to a single glass block. This construction results in a single optical component referred to as the periscope monolith.

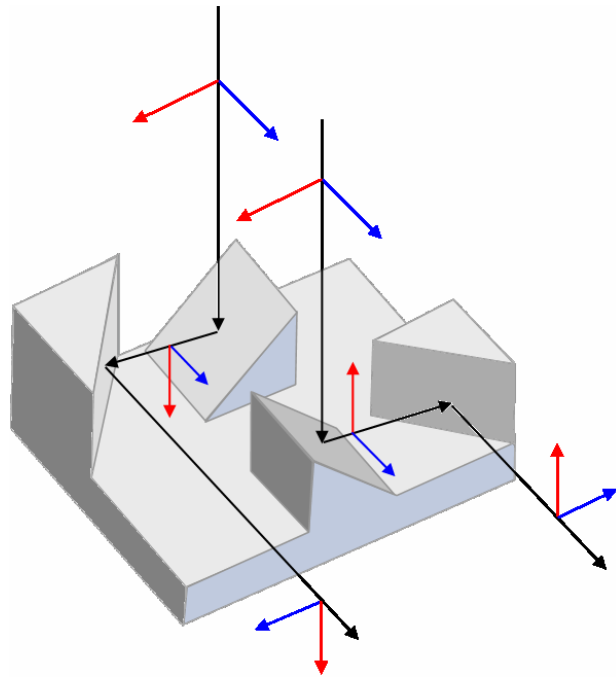


Figure 1 Electric field (pupil) inversion in the periscope nulling architecture.

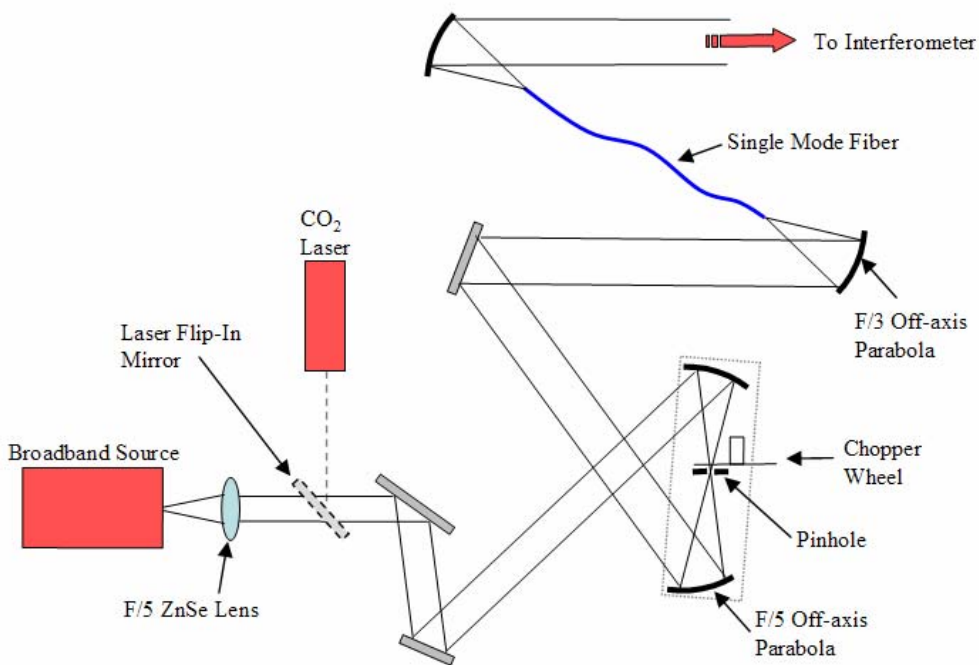


Figure 2. Source and input spatial filter layout.

Interferometer Layout: The sources and input optics, including a single-mode fiber, are shown in Fig. 2. The overall layout of the interferometer is shown in Fig. 3, and a closeup of the input beamsplitter (Beamsplitter 1) and the periscope monolith is shown in Fig. 4. Light from a broadband infrared source is transferred through the single mode fiber, as illustrated in Fig. 2, and directed upward to Beamsplitter 1, shown in Figs. 3 and 4. The two resulting beams are reflected down into the periscope monolith where the electric field inversion is performed. Beam 1 of the interferometer reflects off the piston mirror which is driven by laser metrology for implementation of pathlength (phase) control via picomotor and PZT on a translation stage. The two interferometer beams are combined at Beamsplitter 2 and the null output is transmitted to the output single mode spatial fiber and HgCdTe detector.

Residual Dispersion Compensation: The only non-mirror components that are necessary in the interferometer are two ZnSe beamsplitters. These beam-splitters have, however, a difference of several microns in their respective optical thicknesses because of manufacturing tolerances, and thus introduce a different amount of dispersion in each beam. To compensate for this difference, wedged ZnSe compensator plates are included in each interferometer beam. These plates can be rotated one with respect to the other to match exactly the differential optical thickness due to the beamsplitter mismatch, equalizing the amount of ZnSe in each beam path. The dispersion compensating plates are shown in the interferometer layout of Fig. 3 as “Compensator 1” and “Compensator 2.” Fourier transform spectrometry is used to measure the residual phase dispersion between the interferometer beams.

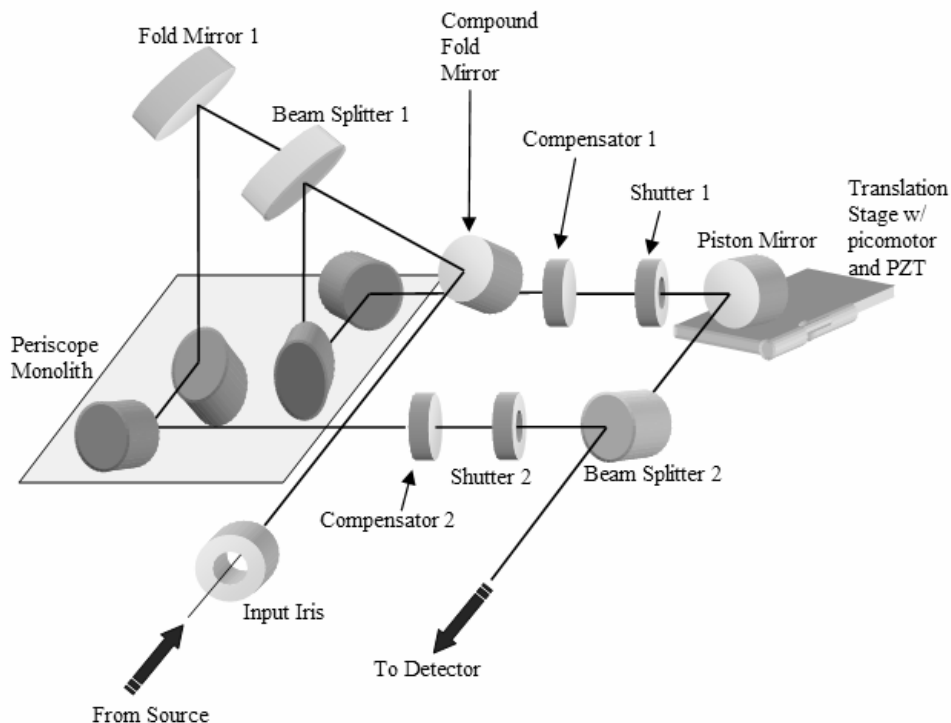


Figure 3. Achromatic Nulling Testbed layout.

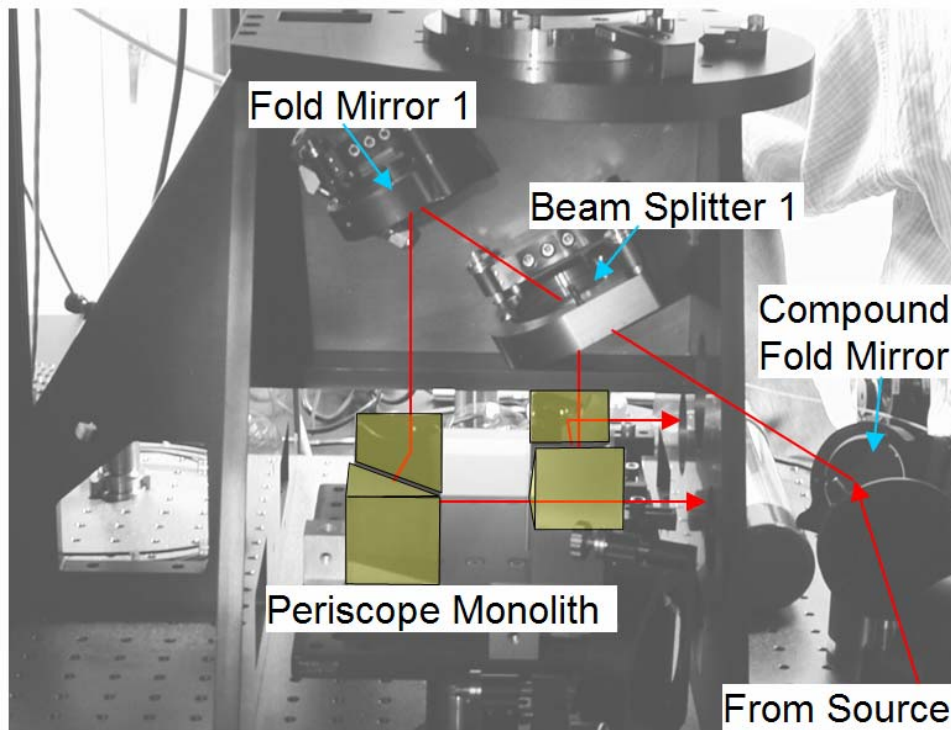


Figure 4. Photograph of the periscope nulling interferometer including Beamsplitter 1 and the field flip mirrors in the periscope monolith.

Spatial Filtering: The full periscope interferometer includes two single mode mid-infrared fibers, made from Chalcogenide glass. The input fiber is used to provide a broadband artificial star that is spatially coherent (i.e. unresolved). As shown in Fig. 2, an off-axis parabolic (OAP) mirror focuses light from the broadband source onto a single mode fiber. The output of this fiber is collimated using another OAP and the beam is steered into the nuller as shown labeled “From Source” in Figures 3 and 4. A second spatial filter is used on the output of the interferometer to reduce sensitivity to tilt and shear within the system. Using a single mode fiber, any tilt errors between the interferometer arms are converted to an intensity mismatch between beams when the beams are coupled into the single mode fiber at the output.

Intensity Matching: Average intensity matching is accomplished through the insertion of thin wires in each beam. Adjustment of the wires allows the average intensity to be controlled to better than 0.25%.

Vibration Isolation: The periscope nulling interferometer has been vibrationally isolated from the building in which it resides through multiple levels of isolation. The interferometer is built on an optical table top which sits on passive air filled isolators on another optical table top. The second table is floated on standard optical table air isolator legs. These tables rest on an isolation pad in the floor which is on a separate foundation from the rest of the building. Finally, the testbed is enclosed in a plexiglass box in order to minimize air turbulence. The vibration isolation results in a residual optical path stability of 2–3 nm rms above 10 Hz.

Path Compensation: During nulling measurements, the optical path difference (OPD) within the interferometer is maintained to within 2–3 nm rms. Although the passive vibration isolation measures effectively minimize the higher frequency OPD effects, a heterodyne metrology system at 633 nm is used to actively control the OPD for frequencies below 10 Hz. The metrology beam is injected through the back side of Beamsplitter 1 slightly decentered from the infrared optical path. The metrology beam is combined with a local oscillator and the resultant signals are detected from the back side of Beamsplitter 2.

2.2. Adaptive Nuller

The adaptive nuller uses a broadband thermal source to generate light with a spectral width $> 3 \mu\text{m}$ in the 7–12 μm wavelength band. This light is put through a simple interferometer with one arm holding the adaptive nuller components, and the other serving as a reference arm. There will be intensity and phase dispersion in this interferometer due to normal manufacturing tolerances which will be compensated by the adaptive nuller.

There is no achromatic phase shifter between the arms of the interferometer. The Adaptive Nuller introduces a half-wavelength delay (approximately 5 microns path difference) and adjusts the residual path difference at each wavelength using the adaptive compensator. The adaptive nuller measures the intensity and phase dispersion as a function of intensity and phase differences between the arms of the interferometer versus wavelength. From this measurement, the required adjustments to the deformable mirror (DM) actuator are calculated and the correction is applied. Through an iterative process the intensity dispersion is corrected to $\leq 0.2\%$ rms (1σ) intensity difference between the arms. The phase dispersion is corrected so that it is $\leq 5\text{nm}$ rms (1σ).

The layout of the Adaptive Nuller has been slightly modified for this milestone. A single-pixel detector is now included at the output of the interferometer so that all the light, normally dispersed in a spectrometer, can be re-directed by a flip-mirror to be focused onto a single pixel for the measurement of a time-series of the null.

Table 1. Comparison of Current Flight Requirements with Pre-Phase A Nulling Testbed Requirements

Parameter	Flight Performance	Achromatic Nuller	Planet Detection Testbed	Adaptive Nuller
Null depth	1×10^{-5}	1×10^{-5}	1×10^{-5}	1×10^{-5}
Amplitude control	0.13%	Derived	0.12%	0.2% (static)
Phase control	1.5 nm	Derived	2 nm	5 nm (static)
Stability timescale	50,000 s +	21,600 s	5,000 s	21,600 s
Bandwidth	83 % (7–17 μm)	25 % (8.3–10.7 μm)	$\lambda = 10.6 \mu\text{m}$	30 % (8.4–11.6 μm)

2.3. Differences between Flight and Lab Demonstration

There are several important differences between the lab demonstration and the baselined flight implementation: 2 beams vs 4 beams, spacecraft dynamics, air vs cryo-vacuum, and the source intensity. Each is addressed briefly below.

2 beams vs 4 beams: the baseline array configuration for TPF-I combines 4 beams to form the null. This is implemented in two stages: pair-wise nulling followed by cross-combination of the two nulled beams. Since all the nulling occurs at the first stage, the two-beam broadband lab demonstrations of the Achromatic Nulling Testbed and the Adaptive Nuller provide a meaningful representation of achievable flight performance. Four-beam combination will then be demonstrated in the lab with the Planet Detection Testbed.

Spacecraft dynamics: a control system is required in flight to stabilize the beams against motions of the spacecraft. It is assumed that the tip/tilt, optical path difference, and shear of each beam is stabilized at the input to the nuller. The lab demonstration has active path length control only. The active stabilization of 4 beams is demonstrated in the Planet Detection Testbed.

Polarization: in the case of the Adaptive Nuller, the flight system will split the two linear polarization states and correct each independently. Both ANT and Adaptive Nuller lab demonstrations operate on unpolarized light without splitting the components, and therefore have fewer degrees of freedom to make a correction.

Cryo-vacuum: the flight system operates in vacuum at low temperature (~ 40 K), compared to the ambient air environment of the lab demonstration. The lab is a more challenging disturbance environment, and the room temperature thermal background is a significant source of noise in the experiment. Future engineering will have to address the need for a DM in the Adaptive Nuller that operates in vacuum at low temperature and the need for cryovacuum compatible pathlength control and dispersion compensation. Other aspects of the design, including the cryogenic stability of the periscope monolith, will also be investigated.

Source intensity: the broadband sources in the lab provide a higher photon flux than the target stars to be observed by the mission. This is offset by the higher detector readout noise in the lab. The goal of this milestone is to demonstrate the fundamental broadband null depth that can be achieved, which is independent of the source intensity. If a 10^5 null is measured with the bright lab source, then the same null would be obtained if the source brightness were suddenly reduced to the level expected from a typical star – but it then wouldn't be measurable in the presence of lab detector noise and the room-temperature background. The source intensity is much more of an issue for the Planet Detection Testbed, which includes pointing and fringe tracking control loops using part of the starlight. In this case, care will be needed to operate the control loops in an SNR regime that is representative of flight.

3. Milestone Procedure: Achromatic Nulling Testbed

3.1. Definitions

The TPF-I M3 broadband starlight suppression demonstration requires measurement and control of an interferometric null. In the following paragraphs we define the terms involved in this process, spell out the measurement steps, and specify the data products.

3.1.1. “Broadband Source”. We define the broadband to be a 60 μm diameter pinhole illuminated with an argon arc source with an equivalent blackbody temperature of 7000–10,000 K. It is a stand-in for the star signal that would have been collected by the telescope systems in TPF-I; however it is not intended to simulate any particular collector design or expected flux.

3.1.2. “Dispersion”. We define dispersion to be the difference in phase as a function of wavelength between the two arms of an interferometer due to a differential glass thickness or mismatched coatings. The differential glass thickness may be due to any glass component (beamsplitters, compensating plates) which are not common path for the two interferometer beams.

3.1.3. “Laser Source”. We define the laser source for ANT to be a carbon dioxide laser with narrow spectral line width that is co-aligned with the broadband source. The laser source is used primarily as an alignment and pathlength stability diagnostic tool. Null depths measured for the laser provide an upper bound for the wavelength independent performance of the interferometer.

3.1.4. “Active metrology”. We define active metrology as a system which uses a laser at 633 nm wavelength to measure the difference in optical paths of the two arms of the interferometer. This information is then fed back to the piston mirror control to maintain a set path difference.

3.1.5 “Interferometer Passband”. We define the passband of the interferometer to be the wavelength range over which nulling measurements are recorded. This passband is established through the use of a transmissive bandpass filter. The full-width-half-max (FWHM) power points of the filter define the passband. The interferometer passband is defined to be the passband width divided by the center wavelength, converted to percent. For example, if a bandpass filter has FWHM power points at 8 μm and 10 μm , then it has a width of 2 μm centered at 9 μm . This yields an interferometer passband of 22%.

3.1.6 “Dispersion Compensation”. Dispersion compensation is defined as the minimization of dispersion, as defined in 3.1.2, which is required to achieve deep broadband nulling. Compensation for this dispersion is accomplished through the introduction of an additional glass plate in each beam. The plates are rotated, changing the glass thickness for the associated beam, to minimize the dispersion.

3.1.7 “Fourier Transform Spectrometry”. We define Fourier Transform Spectrometry (FTS) as the following process used to measure phase dispersion. This process is used iteratively with dispersion compensation to yield minimum phase slope across the interferometer passband. The measurement is performed by scanning the optical pathlength difference of the interferometer through several hundred microns while detecting the broadband interference fringe. The resultant fringe intensity data is Fourier transformed to obtain amplitude and phase versus wavelength. The calculated

phase slope across the passband corresponds directly to the amount of dispersion in the interferometer.

3.1.8 “Null Fringe”. We define the null fringe to be the center of the broadband interference envelope. For a nulling interferometer, this will be a destructive fringe, yielding a minimum power. Null depth is measured at the null fringe.

3.1.9 “Null Depth”. We define null depth to be the ratio of intensity at the constructive fringe peak to the time averaged intensity at the destructive null fringe.

3.2. Measurement of the null

Each null measurement is obtained as follows:

- 3.2.1. The piston mirror is moved to the peak of the constructive fringe. This position is maintained for several seconds to record the average peak power which is used in calculation of the null depth.
- 3.2.2. The piston mirror is then actuated to drive the interferometer to the fringe minimum.
- 3.2.3. The metrology setpoint is scanned to find the minimum total power as measured by the HgCdTe detector.
- 3.2.4. The active metrology control loop holds this set point while the null fringe power is recorded for the duration of the measurement.

3.3. Milestone #3 Validation Procedure

- 3.3.1. The 10 μm laser source, mid-infrared broadband source, and metrology laser source are turned on
- 3.3.2. Relative beam shear is minimized using laser light diffracted from an iris viewed across the pupil at the output of the interferometer.
- 3.3.3. The laser is blocked and the broadband source is opened. The piston mirror is moved to the center of the broadband fringe envelope.
- 3.3.4. Fourier Transform Spectrometry (FTS) measurements are made, as described in Section 3.1.7. The dispersion compensation is optimized to yield a minimum phase slope for FTS results.
- 3.3.5. The piston mirror is again moved to acquire the center of the broadband fringe envelope.
- 3.3.6. Data acquisition is started for the null measurement. The piston mirror is moved to the constructive fringe peak, then returned to the null fringe.

- 3.3.7. The metrology control loop is started and the piston mirror position is adjusted such that the metrology setpoint is centered on the null fringe.
- 3.3.8. The amplitude balance between the interferometer beams is adjusted while holding the null fringe stable with the metrology. The amplitude adjustment is done by moving a small metal wire crosshair into the brighter beam. The null fringe power decreases as the amplitude balance is improved.
- 3.3.9. The time series of the null measurement begins by first moving to the constructive fringe peak, using metrology setpoint control. The peak signal is recorded for 30 seconds.
- 3.3.10. The metrology setpoint control is used to move to the null fringe.
- 3.3.11. The metrology setpoint is held constant for duration of the null measurement.
- 3.3.12. At the end of the null measurement, the metrology control loop is turned off. The shutter in one arm of the interferometer is closed while the other is left open so that the intensity in one arm of the interferometer can be recorded. This is repeated for the other arm. Both shutters are then closed and the residual background and electronic noise is recorded.
- 3.3.13. Data to be included in final report: (a) plot of time series of broadband null depth as specified in Sec. 5, (b) plot of the broadband intensity passing through each arm of the interferometer, measured separately for each arm and showing approximately 600 s of data, (c) plot of the bandpass of the interferometer, shown as the amplitude and phase as a function of wavelength derived from FTS measurements from a single scan through the fringe packet, (d) plot of time series of the laser null depth, showing approximately 600 s of data.

Repeat steps 3.3.1 – 3.3.12 on two more occasions on different days, with at least 48 hours between each demonstration.

4. Milestone Procedure: Adaptive Nuller

4.1. Definitions

The TPF-I M3 broadband starlight suppression demonstration requires measurement of the rejection ratio in an interferometer. In the following paragraphs we define the terms involved in this process, spell out the measurement steps, and specify the data products.

- 4.1.1. **“Star”**. We define the “star” to be a 75 μm diameter pinhole illuminated with ceramic heater thermal source with a temperature of 1250–1570 K. This “star” is the only source of light in the optical path of the adaptive nuller. It is a stand-in for the star signal that would have been collected by the telescope systems in TPF-I; however it is not intended to simulate any particular collector design or expected flux.

- 4.1.2. **“Dispersion”**. We define dispersion to be the difference in either amplitude *or* phase as a function of wavelength between the two arms of an interferometer.
- 4.1.3. **“Algorithm”**. We define the “algorithm” to be the computer code that takes as input the measured amplitude and calculated phase dispersion, and produces as output a voltage value to be applied to each element of the DM, with the goal of reducing the dispersion.
- 4.1.4. **“Cross coupling”**. We define cross coupling to be the unintended adjustment of phase while amplitude is being corrected or the unintended adjustment of amplitude while phase is being corrected.
- 4.1.5. **“Monochromatic source”**. We define a monochromatic source to be a carbon dioxide laser with an operating wavelength near 10 μm with narrow spectral line width that is co-aligned with the “star” source. As we are only able to control dispersion, we do not expect to achieve a null deeper than the null obtained with this source.
- 4.1.6. **“Active metrology”**. We define active metrology as a system which uses a laser at 1.3 μm wavelength to measure the difference in optical paths of the two arms of the interferometer. This information is then fed back to the delay line control to maintain a set path difference.
- 4.1.7. **“Spectrometer”**. We define a spectrometer to be a device to measure intensity as a function of wavelength. The device consists of a grating to disperse the incoming light. The dispersed light is then focused by an off-axis parabola onto a linear mercury cadmium telluride array with 16 elements. Each element produces a voltage proportional to the intensity in a wavelength range selected by the grating. The output voltages are then sent through a multiplexer to a lock-in amplifier with an integration time set from 100 ms to 30 s depending on the signal level. The output of the lock-in amplifier is then read by the computer for each element of the linear array. Noise may be reduced by averaging up to 10 frames taken from the spectrometer.
- 4.1.8. **“Single Pixel Detector”**. We define the single-pixel detector to be a single mercury cadmium telluride detector, which can be used in parallel with the spectrometer. A pick-off mirror placed before the grating directs the undispersed light from the single mode spatial filter to be focused on this detector.
- 4.1.9. **“Adaptive nulling”**. We define the process of adaptive nulling to be the following 4 step process, iteratively repeated for as many cycles as necessary to reach the desired level of amplitude and phase dispersion.
- Measure the intensity dispersion in the interferometer by measuring the intensity spectrum of each arm independently while shuttering off the other arm.
 - Compute the required tilts to equalize the intensity difference in each channel of the deformable mirror (DM) and apply these voltages.
 - Calculate the phase dispersion in the interferometer by actuating the delay line several fringes off the null and measuring the dispersed spectral fringes with the spectrometer and applying an algorithm to the output.
 - Compute the required piston settings to equalize the path lengths in each channel of the DM and apply these voltages.

4.1.10. “Null Depth”. We define the null depth to be the ratio of the peak signal caused by constructive interference in the interferometer to the null signal caused by destructive interference in the interferometer.

4.1.11. “Rejection Ratio”. We define the rejection ratio to be the inverse of the null depth.

4.2. Measurement of the null

Each null measurement is obtained as follows after intensity and phase correction have been applied:

4.2.1. The delay line is actuated by the computer to locate the approximate position of the minimum integrated power as measured on the single pixel detector.

4.2.2. The delay line is then actuated by the computer to the peak integrated power. The set point is slowly scanned on the active metrology to locate the peak. The peak integrated power is used to normalize the null depth.

4.2.3. The delay line is then actuated by the computer back to the null.

4.2.4. The metrology set point is then slowly scanned by the computer to find the minimum integrated power as measured on the single-pixel detector.

4.2.5. The active metrology system can then be used to hold this position to measure the time evolution of the null.

4.3. Milestone #3 Validation Procedure

4.3.1. All DM actuators are set to half their control range.

4.3.2. The active metrology system and the star are turned on. The delay line is then actuated by the computer to locate the null position.

4.3.3. An initial uncorrected null is measured as described in Sec. 4.2.

4.3.4. The delay line is actuated away from the null by several fringes and adaptive nulling is performed to correct the measured intensity dispersion to $\leq 0.2\%$ and correct the measured phase dispersion to $\leq 5\text{nm}$.

4.3.5. The delay line is actuated by the computer to locate the null position.

4.3.6. The corrected null is measured as described in Sec. 4.2

4.3.7. To measure the stability, step 4.3.6 is repeated while the DM voltages are held constant and the active metrology holds the delay line position to measure the time evolution of the null.

- 4.3.8.** The following data are to be archived for future reference: (a) raw spectrometer output of null and peak of star before and after correction, (b) phase and intensity dispersion before and after correction, and (c) raw output of the null and peak measured at each time interval after correction.
- 4.3.9.** The following data are to be presented in the final report: (a) Plot showing peak and null as a function of wavelength before and after correction, (b) plot of time series of null depth.
- 4.3.10.** Repeat steps 4.3.1 – 4.3.7 on two more occasions on different days, with at least 48 hours between each demonstration.

5. Success Criteria

The following is a statement of the 3 elements that must be demonstrated to close the TPF-I M3. Each element includes a brief rationale. The success criteria are common to both the Achromatic Nulling Testbed and the Adaptive Nuller. However, the Milestone criteria need only be met by one of the two testbeds in order to close the Milestone.

- 5.1** A null depth measured over a fractional bandwidth of $\Delta\lambda/\lambda \geq 25\%$, where the central wavelength, λ , lies in the range $7 \mu\text{m} < \lambda < 12 \mu\text{m}$.

Rationale: The bandwidth is large enough to give confidence that a small number of instruments would be necessary to cover the full TPF-I science band of 7–18 μm .

- 5.2** A time series showing mean null depth to be less than or equal to 1×10^{-5} observed in single or dual-polarization light for a 6 hour period. The mean null depth is defined as the average measured power at the null fringe over a contiguous 6 hour time period. The data from which the average is estimated will be a continuous data set, without gaps, that spans at least a 6-hour period. Although the null depth may be allowed to exceed 1×10^{-5} for long periods, the average as measured over the entire 6 hours must be less than or equal to 1×10^{-5} . The brightness of the experimental source need not be representative of a typical stellar source. The room temperature will be monitored but not controlled beyond the facility controls for the room.

Rationale: The null depth to be demonstrated is the flight requirement and would allow planet signal extraction when methods of instability noise compensation are employed. As this milestone emphasizes broadband performance, a single-polarization measurement is sufficient; dual-polarization performance, if not demonstrated here, will be addressed in a subsequent milestone. The null depth is independent of the source brightness, and thus there is no requirement imposed for the use of representative light levels for this milestone. A representative science observation would require an array rotation period of 50,000 s (~14 hrs), and thus the time-series duration of 6 hrs demonstrates long-term stability of the system, approaching flight-level requirements.

- 5.3** Elements 5.1 – 5.2 must be satisfied simultaneously on three separate occasions with at least 48 hours between each demonstration.

Rationale: This provides evidence of the repeatability of the broadband starlight suppression.

6. Certification Process

The TPF-I Project will assemble a milestone certification data package for review by the EIRB. In the event of determination that the success criteria have been met, the project will submit the finding of the review board, together with the certification data package, to NASA HQ for official certification of milestone compliance. In the event of disagreement between the project and the EIRB, NASA HQ will determine whether to accept the data package and certify compliance or request additional work.

6.1. Certification Data Package

The milestone certification data package will contain the following explanations, charts, and data products.

- 6.1.1. A narrative report, including a discussion of how each element of the milestone was met, an explanation of each plot or group of plots, appropriate tables and summary charts, and a narrative summary of the overall milestone achievement.
- 6.1.2. Although the body of the report will document the performance of the testbed that met the milestone requirements, the report will also include an appendix to document the performance of the other testbed. This appendix is not included as part of the success criteria, but is for completeness and information only.

7. References

- R.O. Gappinger, R.T. Diaz, S.R. Martin, F.M. Loya, P.R. Lawson, “Current progress on TPF-I mid-infrared achromatic nulling at the Jet Propulsion Laboratory,” Proc. SPIE **6693**, 669318 (2007).
- A. Ksendzov, E. Bloemhof, V. White, J. K. Wallace, R. O. Gappinger, J. S. Sanghera, L. E. Busse, W. J. Kim, P. C. Pureza, V. Q. Nguyen, I. D. Aggarwal, S. Shalem, and A. Katzir, “Measurement of spatial filtering capabilities of single mode infrared fibers,” in *Advances in Stellar Interferometry*, J. D. Monnier, M. Schöller, and W. C. Danchi, Editors, Proc. SPIE **6268**, 626838 (2006).
- P. R. Lawson and J. A. Dooley, Editors, *Technology Plan for the Terrestrial Planet Finder Interferometer*, JPL Pub 05-5 (Jet Propulsion Laboratory: Pasadena, CA, 2005).
<http://planetquest.jpl.nasa.gov/Navigator/library/tpf1414.pdf>
- Oliver P. Lay, “Removing instability noise in nulling interferometers”, Proc. SPIE **6268**, 62681A (2006)
- Robert D. Peters, Oliver P. Lay, Akiko Hirai, Muthu Jeganathan, “Adaptive nulling in the mid-IR for the Terrestrial Planet Finder Interferometer,” in *Techniques and Instrumentation for Detection of Exoplanets III*, D. R. Coulter, Editor, Proc. SPIE **6693**, 669315 (2007).